Proceedings of the 1996 IEEE
International Conference on Robotics and Automation
Minneapolis, Minnesota - April 1996

Gait Kinematics for a Serpentine Robot

Jim Ostrowski
School of Engineering and Applied Science
University of Pennsylvania
297 Towne Bldg., 220 S. 33^{rd} St.
Philadelphia, PA 19104-6315
Email: jpo@robby.caltech.edu

Joel Burdick
Division of Engineering and Applied Science
California Institute of Technology,
Mail Code 104–44
Pasadena, CA 91125
Email: jwb@robby.caltech.edu

Abstract: *This paper considers the problem of serpentine, or snake-like, locomotion from the perspective of geometric mechanics. A particular model based on Hirose's Active Cord Mechanism (ACM) is analyzed. Using the kinematic constraints, we develop a* connection, *which describes the net motion of the machine as a function of variations in the mechanism's shape variables. We present simulation results demonstrating three types of locomotive gaits, one of which bears an obvious resemblance to the serpentine motion of a snake. We also discuss how these algorithms can be used to optimize certain inputs given the particular choice of physical parameters for a snake robot.*

1. Introduction

Most mobile robots are wheeled vehicles, since wheels provide the simplest means for robotic mobility. The assumption that these wheels do not slip provides nonholonomic kinematic constraints on a vehicle's motion. These kinematic nonholonomic systems have been extensively studied in the literature. For more rugged terrains, robotics researchers have also considered legged robot designs. Nature, however, has demonstrated that there are a significant number of alternative forms of locomotion, each one suited to a different purpose and scale of motion. Examples include swimming, flying, sliding, burrowing, etc. Just as nature uses evolution to tailor each of these types of motion to their environments, so also have modern roboticists examined alternative forms of locomotion suited to particular problems. This paper focuses one such mode of robotic locomotion, namely snake-like, or serpentine, locomotion.

One of the original studies of snake-like robots was conducted by Hirose [1, 2], who approached the problem from a biologically inspired point of view. Hirose formulated what he termed a *serpenoid* curve—a curve representing the path that a snake would trace out as it slithers forward using an *undulatory* gait. He also showed that a snake-like vehicle could generate a net forward force by applying the appropriate torques along the length of its body. Using these results, he successfully built a wheel-based, snake-like robot capable of propelling itself forward using only internal torques (that is, without directly driving the wheels). The robot (see Figure 1, photo taken from [1]), called the Active Cord Mechanism Model 3 (ACM III), consisted of a long chain of serially connected segments, each of which sat upon an actively controlled, rotating wheel base (the wheels are designed to act like the belly of a snake in preventing lateral slipping). However, the control of the robot's position remained a heuristically derived procedure, without the ability to give precise feedback control for this form of locomotion.

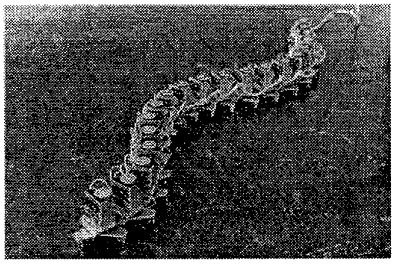

Fig. 1: The Active Cord Mechanism (ACM III)

More recently, Chirikjian and Burdick [3] coined the term *hyper-redundant* to describe robots with a very large number of independent degrees of freedom. Naturally, snake robots fall into this category. Chirikjian and Burdick considered locomotion schemes that were reminiscent of the sidewinding [4] and creeping [3] gaits of snakes. They also considered gaits that are analogous to those of inchworms and earthworms. However, a complete analysis and understanding of the *undulatory* gait of snakes has yet to be attained.

Tsakiris and Krishnaprasad [5] have also used the same Variable Geometry Truss (VGT) mechanism employed by Chirikjian and Burdick to develop models that employ no-slip wheel constraints and can be used to generate locomotion patterns. They term these models "G-snakes," in reference to the notion that each segment must move within a constrained subset of a Lie group, G. They have shown that gaits (i.e., specified input patterns) can be explicitly integrated to describe the overall locomotory motion. Kelly and Murray [6] have modelled a large number of locomotive systems, including basic inchworm and sidewinding gaits (using a viscous friction model). They have derived results for determining controllability, as well as suggestions for the generation of locomotive walking patterns, or *gaits*.

0-7803-2988-4/96 $4.00 © 1996 IEEE

The intent of this paper is to show how the analysis of the undulatory gait can be formulated in terms of some of the intrinsic properties found in general modes of locomotion. Recent work [6, 7, 8, 9] has shown that for a large class of locomotive systems there exists a basic underlying mathematical framework. This extra structure can be exploited to gain a better understanding of the processes of locomotion. In the present context, we seek to use these tools to explore the undulatory gait. In doing so, we hope to demonstrate theoretically how to implement locomotion schemes which to date were found purely heuristically, and to add additional gaits that may not have been realized in previous works.

2. Background

In [8] we described a general framework for studying the mechanics of undulatory locomotion systems. We review here the relevant aspects of this work, in order to motivate the use of this geometrical framework in the study of more general problems of locomotion.

It is always possible to divide a locomoting robot's configuration variables into two classes. The first class of variables describes the *position* of the robot relative to an inertial frame. Since robots move in Euclidean space, the set of frame displacements is $SE(m), m \leq 3$, or one of its subgroups—i.e., a Lie group. For our purposes, we will primarily be interested in $SE(2)$, the group of translations and rotations in the plane. The second class of variables defines the internal configuration, or *shape*, of the mechanism. We only require that the set of all possible shapes (the "shape space") be described by a manifold, M. Hence, the Lie group, G, together with the shape space, M, form the total configuration space of the system, which we denote by $Q = G \times M$.

We say that Q is a *fiber bundle* with *fibers* (position) G and *base space* (shape space) M. When the fibers are Lie groups (as is the case here using position variables), this splitting of configuration variables into position and shape describes a *principal fiber bundle*. The group variables have a natural translation, or *action*, denoted by L_g, such that $L_g h = gh$ for $g, h \in G$ (for problems of locomotion, this is most commonly represented by matrix multiplication on the left). The action on G naturally extends to an action Φ_g on Q by $\Phi_h(g, r) = (L_h g, r)$ for $(g, r) = q \in Q$ (this is sometimes denoted by simply $h \cdot q$). The tangent map of Φ_g, denoted $T_q\Phi_g$, is called the *lifted action* of G on Q. The interpretation of the configuration space as a principal bundle has been successfully used for kinematic locomotion systems by Kelly and Murray [6] and for dynamic systems implicitly by Montgomery [10] and explicitly by Ostrowski et al. [7, 8].

The shape and position variables are coupled by the constraints acting on the robot. Hence, by making changes in the shape variables, it is possible to effect changes in the position variables through the constraints. The relationship between shape changes and position changes can be described using a geometric quantity called a *connection*. The mathematical properties of connections allow us to simplify greatly both the dynamics *and* the control of locomotion systems.

In accordance with the literature, let us denote by V_qQ the *vertical subspace* composed of all vectors are tangent to the fiber. That is, a vector $v_q \in V_qQ$ represents a net velocity of the body with respect to an inertial frame, such that $v_q = (v_g, 0)$ with $v_g \in T_gG$. We then define the connection to be the invariant *horizontal subspace* composed of those vectors complementary to VQ that correctly represent the interaction between shape and position velocities as specified by the constraints.

Definition 1 *A* connection *is a smooth assignment of a* horizontal subspace, $H_qQ \subset T_qQ$, *for each point* $q \in Q$ *such that*

1. $T_qQ = V_qQ \oplus H_qQ$, *and*
2. $T_q\Phi_g H_qQ = H_{g \cdot q}Q$, *for every* $q \in Q$ *and* $g \in G$.

A connection can alternatively be written locally as a Lie algebra-valued one-form, i.e., a mapping $\mathbb{A}(r) : T_rM \to \mathfrak{g}$, where elements in $\mathfrak{g}$ (which can be thought of as screws) describe translational and rotational velocities relative to a frame attached to the robot. $\mathbb{A}$ is said to be the *local form* of the connection, such that if $\dot{q}$ is a horizontal velocity vector, with $\dot{q} = (\dot{g}, \dot{r})$, then $\dot{q}$ must satisfy the relationship

$$g^{-1}\dot{g} = -\mathbb{A}(r)\dot{r}, \tag{2.1}$$

where $g^{-1}\dot{g} = T_gL_{g^{-1}}\dot{g} \in \mathfrak{g}$. Notice that as a map from shape velocities to position (fiber) velocities, $\mathbb{A}$ provides most (and in some cases all) of the information required to understand the effect of internal shape changes in generating locomotion.

The analysis contained in this paper focuses on a kinematic system in which dynamics do not play a significant role. It should be noted, however, that a locomoting robot will in general be subject to two types of constraints: kinematic and dynamic. The kinematic constraints typically arise from kinematic rolling and/or slipping assumptions. For example, a wheeled based robot has no-slip constraints along the wheel axes. The dynamic constraints arise from symmetries, or invariances, of the Lagrangian with respect to the group action, Φ_g. In the case of locomotion, these constraints are conservation laws, such as conservation of linear or angular momentum. However, when both constraints are present, the kinematic constraints may break some or all of the system's symmetries.

In [8] we develop a methodology to construct a connection in the general case of mixed constraints which

can be used to study problems of *dynamic* locomotion. The form of the connection in both cases leads us to the following observation regarding locomotion systems: the dynamics and the constraints are in general invariant with respect to the action of the Lie group. Thus, the relative effect of a wheel constraint remains unchanged under transformations of position and orientation as do the inertial properties of the system. It is this invariance that allows us to write the connection in the form of Eq. 2.1.

3. The Kinematic Snake Model

The system presented here is based on the ACM III snake robot built by Hirose [2], where certain assumptions are made regarding the actuation of the individual segments. The basic principles relating the ACM III to a real snake are based on the idea that the body of a real snake has a small coefficient of friction along the length of its belly and a high coefficient of friction transverse to its length. Discretization of the snake's backbone curve then allows us to model the snake as a finite number of such wheeled segments. The reader is referred to [1] for more detail.

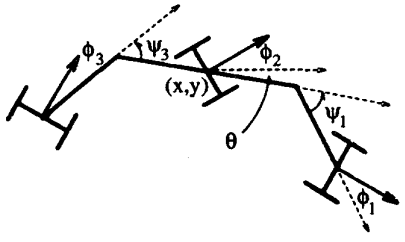

Fig. 2: A model for the kinematic snake

We begin by examining a three-segment model of a snake (see Figure 2). We find that there are the same number of constraints as the dimension of G, and so the kinematic constraints define a connection. This is called the *principal kinematic case*, and is studied for other locomotion systems by Kelly and Murray in [6]. We assume that there are control inputs at each segment joint and at each wheel pivot joint. The wheels themselves are unactuated and rotate freely.

Recognizing that the three wheel constraints define a connection leads naturally to a method for handling additional body segments. The technique consists of using the first three segments to define the motion in $SE(2)$, and then using the wheel constraints of the additional bays as the governing equations for these segments. Thus, we develop a system that has a "following" behavior, in which the lead segments define the path to be traced, and the additional segments are constrained to follow this lead. In a real snake, the additional segments serve a useful purpose in providing greater stability for the snake, and can be used to perform more complicated maneuvers, such as crossing over gaps in the floor or pushing off objects to move along a slippery surface.

For the three segment snake drawn in Figure 2, we label the center point of the middle segment by $(x, y, \theta) \in SE(2)$, the wheel angles of segments 1, 2, and 3 by $(\phi_1, \phi_2, \phi_3) \in \mathbb{S} \times \mathbb{S} \times \mathbb{S}$, respectively, and the relative orientation of segment 1 with respect to segment 2 and segment 2 with respect to segment 3 by $(\psi_1, \psi_3) \in \mathbb{S} \times \mathbb{S}$, respectively.

Each no-slip wheel constraint takes the following general form:

$$(-\sin\tilde{\phi}_i, \cos\tilde{\phi}_i) \cdot \begin{pmatrix} \dot{\bar{x}}_i \\ \dot{\bar{y}}_i \end{pmatrix} = 0,$$

where $\tilde{\phi}_i$ is the absolute angle (measured with respect to horizontal) of the i^{th} wheel, and $(\bar{x}_i, \bar{y}_i)$ is the Cartesian positioning of the center of rotation for the i^{th} wheel. Using this notation, we find that

$$\begin{aligned}
\bar{x}_1 &= x + l\cos\theta + l\cos(\theta - \psi_1), \\
\bar{y}_1 &= y + l\sin\theta + l\sin(\theta - \psi_1), \\
\bar{x}_2 &= x, \qquad \bar{y}_2 = y, \\
\bar{x}_3 &= x - l\cos\theta - l\cos(\theta + \psi_3), \\
\bar{y}_3 &= y - l\sin\theta - l\sin(\theta + \psi_3),
\end{aligned}$$

and $\tilde{\phi}_1 = \phi_1 - \psi_1 + \theta$, $\tilde{\phi}_2 = \phi_2 + \theta$, and $\tilde{\phi}_3 = \phi_3 + \psi_3 + \theta$. Thus, the constraint equations can be written as

$$\begin{aligned}
&-\sin\tilde{\phi}_1\,\dot{x} + \cos\tilde{\phi}_1\,\dot{y} \\
&\qquad -l(\cos\phi_1 + \cos(\phi_1 - \psi_1))\dot{\theta} = -l\cos\phi_1\,\dot{\psi}_1, \qquad (3.2) \\
&\qquad -\sin\tilde{\phi}_2\,\dot{x} + \cos\tilde{\phi}_2\,\dot{y} = 0, \qquad (3.3) \\
&-\sin\tilde{\phi}_3\,\dot{x} + \cos\tilde{\phi}_3\,\dot{y} \\
&\qquad -l(\cos\phi_3 + \cos(\phi_3 + \psi_3))\dot{\theta} = l\cos\phi_3\,\dot{\psi}_3, \qquad (3.4)
\end{aligned}$$

This supplies three constraints on the three dimensional Lie group, $G = SE(2)$. Straightforward calculations show that the constraints are G-invariant. Therefore, the kernel of these constraints defines a connection on the trivial principal fiber bundle $Q = G \times M = SE(2) \times \mathbb{S} \times \mathbb{S} \times \mathbb{S} \times \mathbb{S} \times \mathbb{S}$. We can invert the constraint equations directly to write the local form of the connection one-form as

$$\xi = g^{-1}\dot{g} = -\mathbb{A}(r)\dot{r}, \xi \in \mathfrak{g}.$$

This gives the following:

$$\xi^1 = -\frac{l^2 \cos\phi_2}{\det W}\big[\dot\psi_1 \cos\phi_1 (\cos(\phi_3 - \psi_3) + \cos\phi_3) + \dot\psi_3 \cos\phi_3 (\cos(\phi_1 + \psi_1) + \cos\phi_1)\big] \tag{3.5}$$

$$\xi^2 = -\frac{l^2 \sin\phi_2}{\det W}\big[\dot\psi_1 \cos\phi_1 (\cos(\phi_3 - \psi_3) + \cos\phi_3) + \dot\psi_3 \cos\phi_3 (\cos(\phi_1 + \psi_1) + \cos\phi_1)\big] = \xi^1 \tan\phi_2 \tag{3.6}$$

$$\xi^3 = \frac{l}{\det W}\big[\dot\psi_1 \cos\phi_1 \sin(\phi_3 + \psi_3 - \phi_2) - \dot\psi_3 \cos\phi_3 \sin(\phi_1 - \psi_1 - \phi_2)\big], \tag{3.7}$$

where

$$\det W = l[\sin(\phi_1 - \psi_1 - \phi_2)(\cos(\phi_3 + \psi_3) + \cos\phi_3) + \sin(\phi_3 + \psi_3 - \phi_2)(\cos(\phi_1 - \psi_1) + \cos\phi_1)].$$

Next, we examine a possible method for extending the snake to an arbitrary number of segments. Suppose that we add a fourth segment. Let ϕ_4 and ψ_4 denote the angles of the wheels and the body segment, respectively. Then, following the above notation,

$$\tilde\phi_4 = \phi_4 + \psi_3 + \psi_4 + \theta,$$
$$\bar x_4 = x - l\cos\theta - 2l\cos(\theta + \psi_3) - l\cos(\theta + \psi_3 + \psi_4),$$
$$\bar y_4 = y - l\sin\theta - 2l\sin(\theta + \psi_3) - l\sin(\theta + \psi_3 + \psi_4),$$

and the constraint becomes

$$-\sin\tilde\phi_4\,\dot x + \cos\tilde\phi_4\,\dot y - l(\cos(\phi_4 + \psi_3 + \psi_4) + 2\cos(\phi_4 + \psi_4) + \cos\phi_4)\dot\theta - l(2\cos(\phi_4 + \psi_4) + \cos\phi_4)\dot\psi_3 = l\cos\phi_4\,\dot\psi_4. \tag{3.8}$$

Observe that we have added two additional degrees of freedom— one wheel angle, ϕ_4, and one inter-segment angle, ψ_4— and added one kinematic constraint given by Eq. 3.8. As with the first three body segments, we will control both ϕ_4 and ψ_4, but now are forced to satisfy the constraint as well. This is easily done, however, by choosing to control the wheel angle, while inverting Eq. 3.8 to give a governing equation for ψ_4. Thus,

$$\dot\psi_4 = \frac{1}{\cos\phi_4}\Big(\frac{1}{l}(-\sin\tilde\phi_4^e\,\xi^1 + \cos\tilde\phi_4^e\,\xi^2) - (\cos\tilde\phi_4^e + 2\cos(\phi_4 + \psi_4) + \cos\phi_4)\xi^3 - (2\cos(\phi_4 + \psi_4) + \cos\phi_4)\dot\psi_3\Big),$$

where $\tilde\phi_4^e = \phi_4 + \psi_3 + \psi_4$, i.e., $\tilde\phi_4^e = \tilde\phi_4\big|_{g=e} = \tilde\phi_4\big|_{\theta=0}$. Notice that the process of solving for $\dot\psi_4$ yields a term with $\cos\phi_4$ in the denominator, which is always nonzero since we assume that the wheels cannot pivot to an angle of $\pm\frac{\pi}{2}$.

Repeating this process, we can add as many additional segments as desired, with the guarantee that each of the following segments properly satisfy all of the constraints. One point to notice is that as we continue to add constraints, it is always possible to arrange the additional constraint equations in the following form:

$$B(\phi_4, \ldots, \phi_k)\begin{pmatrix}\dot\psi_4\\ \vdots\\ \dot\psi_k\end{pmatrix} = C(\phi_4, \ldots, \phi_k, \psi_3, \ldots, \psi_k)\begin{pmatrix}\xi\\ \dot\psi_3\end{pmatrix},$$

where k is the total number of body segments for the snake. The matrix B is lower triangular, with $\det(B) = \prod_{j=4}^{k} l\cos\phi_j$, and so is always invertible.

4. Locomotive Gaits

With the kinematic snake of Hirose, there is obviously a principal gait pattern in which we are most interested— the undulatory gait found in common snakes as they slide along the ground. This gait was described by Hirose as being closest to a "serpenoid" curve, which we show below to be strikingly similar to the patterns generated by our theoretical model. We also present two other gaits not normally seen in nature, but which could be implemented in a snake robot based on Hirose's ACM III.

One of the challenges in working with this model stems from the presence of singularities. These occur any time a pair of the wheel axes intersect at a point. This occurs frequently for the gaits we are examining, and forces us to choose carefully the form of the input functions. Further work is obviously necessary, perhaps with extensions to include slipping of the wheels.

The gaits presented below are only a selection of the more interesting gaits that have been explored. They are all based on integrally related frequencies of the shape inputs. The ratios we give relate the frequency of bending of the inter-segment angle ψ_i to the frequency of the rotation of the wheels, measured by ϕ_i. Thus, a 2:1 gait represents the segments bending at twice the speed as the turning of the wheels. The relative phasing of each of these angles will play a critical role in generating locomotion.

The "serpentine" gait

We begin the analysis by examining the serpentine gait arising from a 1:1 frequency ratio. For this, we use sinusoidal inputs:

$$\phi_i = a_i^\phi \sin(\omega_i^\phi t + p_i^\phi),$$

where similar values for ψ_i are superscripted with a ψ. The parameter values chosen for the simulations (Figure 3) were

$$a_1^\phi = a_3^\phi = 0.2 = -a_2^\phi, \qquad a_1^\psi = a_3^\psi = 0.6,$$
$$\omega_1^\phi = \omega_2^\phi = \omega_3^\phi = 1, \qquad \omega_1^\psi = \omega_3^\psi = 1,$$

with the length of each segment set to 0.2m.

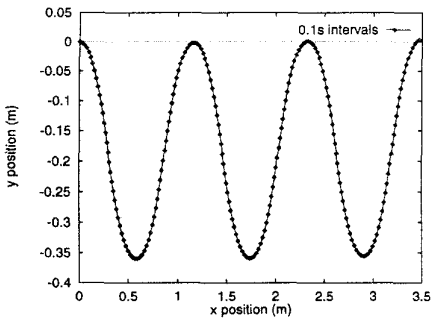

Fig. 3: A plot of (x, y) for the kinematic snake in serpentine mode

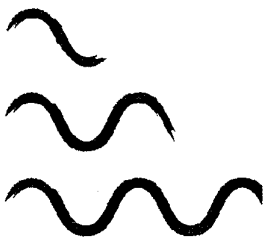

Fig. 4: A trace of the kinematic snake in serpentine mode

For the phasing, we send a traveling wave down the length of the snake (by incrementing the phase of the wheels at each segment), while forcing the inter-segment angle, ψ_i, to move $\frac{\pi}{2}$rad out of phase with their corresponding wheels. Thus, for the simulation shown in Figure 3, the phases are given by

$$p_1^\phi = -\tfrac{\pi}{16}, \quad p_2^\phi = 0, \quad p_3^\phi = \tfrac{\pi}{16},$$
$$p_1^\psi = \tfrac{7\pi}{16}, \qquad\qquad p_3^\psi = \tfrac{9\pi}{16}.$$

Notice that each of the wheel angles differs by $\frac{\pi}{16}$, while the joint angles are $\frac{\pi}{2}$ out of phase of their respective wheel angles. To give an idea of how this resembles the motion of a snake, we include a trace of the serpentine motion in Figure 4.

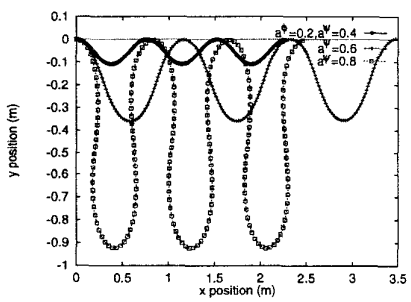

Fig. 5: Three different shapes for the serpentine gait

By varying the magnitudes of the wheel angles (or the inter-segment joint angles), slightly different patterns of locomotion occur. Figure 5 shows the resultant gaits for three different values of $a_1^\psi = a_3^\psi = a^\psi$. Each simulation is run for the same length of time,

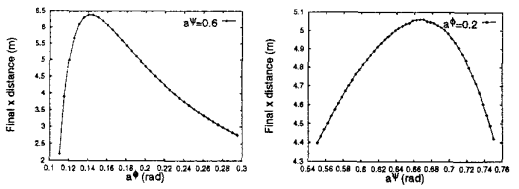

Fig. 6: Joint angle parameter sweeps versus "forward" distance traveled

which indicates that certain parameter values will result in a greater overall distance being traveled. This observation can be very useful in designing an actual snake robot by helping to optimize the parameters chosen for locomotion. In Figure 6 we present two parameter sweeps which show obvious peaks indicating possible optimal parameter choices, given the phasing between segments ($\frac{\pi}{16}$rad) and segment length (0.2m).

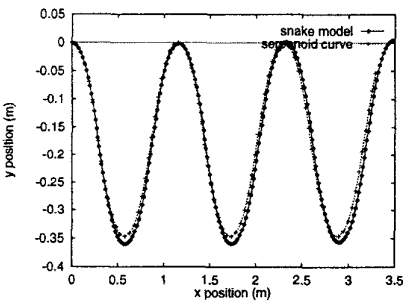

Fig. 7: A comparison of the kinematic snake model versus the serpenoid curve

One point of interest is to examine how this motion compares with the serpenoid curve proposed by Hirose [1]. We generate this curve using the following parameterization:

$$\dot{x} = \cos\left(\alpha \sin(\beta s)\right) \tag{4.9}$$
$$\dot{y} = -\sin\left(\alpha \sin(\beta s)\right). \tag{4.10}$$

The parameters α and β can be chosen such that the serpenoid curve can be made to match arbitrarily closely any of the serpentine patterns of the 1:1 gait. An example of this is given in Figure 7, with $\alpha = 0.85$ and $\beta = \frac{23\pi}{16} \simeq 4.52$rad.

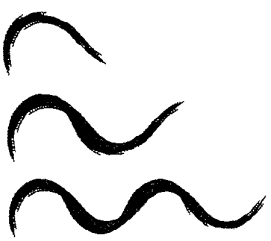

Fig. 8: Traces of the 5-link kinematic snake

As a final note on the serpentine gait, we mention that it appears to work well when additional segments are added using the methods described above. This is a qualitative statement based on the trace of the

5-segment robot given in Figure 8. Further analysis will explore the feasibility of employing additional segments when following other patterns of motion.

The "rotate" gaits

Finally, there are two other types of gaits, both producing a net rotation, albeit using very different types of motion. A 2:1 gait uses a more "natural" type of gait for a snake, characterized by forward and backward motions, reminiscent of how humans turn a car in tight situations, e.g., a "three-point turn." This gait is shown in Figure 9 with the same parameters except for joint magnitudes, $a_1^\phi, \ldots, a_5^\phi$ and a_1^ψ, a_2^ψ, being set to 0.4 and 0.5, respectively.

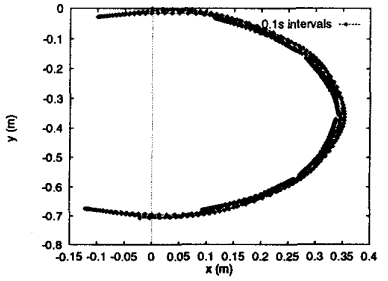

Fig. 9: A trace of the central segment for the 2:1 gait

Alternatively, a 1:2 gait exists for this type of robot. Although the motion does not seem practical for a real snake, it could be employed by a mobile robot. Finally, the 1:2 rotate gait, with the parameters set so that $a^\phi = \frac{\pi}{4}$ and $a^\psi = \frac{3\pi}{8}$, is shown in Figure 10. Notice that we have plotted the variation of θ, the angle of the central body segment, with respect to time. This is because the actual (x, y) position of this segment moves only very insignificantly during the motion of this gait.

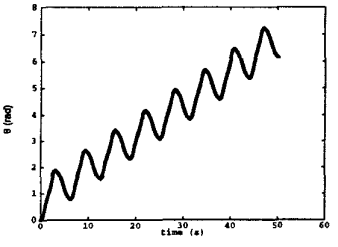

Fig. 10: A trace of the angle θ for the 1:2 gait

5. Discussion and Conclusions

We have examined a model for a snake robot based on the ACM III built by Hirose. By using the intrinsic invariances of the constraints, we can realize the three-segment model as a principal kinematic system. The three wheel constraints define a kinematic connection and so fully determine the effect of internal shape changes on net serpentine locomotion. We utilize this fact to control additional segments which are constrained to "follow" the lead of the three-segment kinematic system.

By formulating the motion of the system in terms of a connection, we can clearly highlight the important factors which contribute to the serpentine locomotion. Using sinusoidal inputs which are phase-delayed down the length of the snake robot, we were able to simulate various possible gaits, including a serpentine gait and two rotate gaits. We showed that the serpentine gait very closely approximates the serpenoid curve developed by Hirose.

The next logical step for this research is to begin to ask deeper questions regarding controllability of snake-like robots. We have shown here basic motions that can be generated, but can not conclude how to specify more general gait patterns (for example, we have yet to find a gait pattern that generates motion transverse to the length of the snake). Kelly and Murray [6] have given initial constructive controllability tests based on taking derivatives of the connection, $\mathbb{A}$ (similar to taking Lie brackets of the input control vector fields). These results will need to be taken further, however, perhaps by examining the relationship between the directions given by Lie brackets and the corresponding gait patterns generated using integrally related sinusoidal inputs.

References

[1] S. Hirose, *Biologically Inspired Robots: Snake-like Locomotors and Manipulators.* Oxford: Oxford University Press, 1993. Translated by Peter Cave and Charles Goulden.

[2] S. Hirose and A. Morishima, "Design and control of a mobile robot with an articulated body," *The International Journal of Robotics Research*, vol. 9(2), pp. 99–114, 1990.

[3] G. S. Chirikjian and J. W. Burdick, "Kinematics of hyper-redundant locomotion with applications to grasping," in *Proc. IEEE Int. Conf. on Robotics and Automation*, (Sacramento, CA), pp. 720–727, April 1991.

[4] J. W. Burdick, J. Radford, and G. S. Chirikjian, "A sidewinding locomotion gait for hyper-redundant robots," in *IEEE Int. Conf. on Robotics and Automation*, (Atlanta, GA), pp. 101–106, May 1993.

[5] P. S. Krishnaprasad and D. P. Tsakiris, "*G*-snakes: Nonholonomic kinematic chains on Lie groups," in *Proc. 33rd IEEE Conf. on Decision and Control*, (Lake Buena Vista, FL), December 1994.

[6] S. D. Kelly and R. M. Murray, "Geometric phases and locomotion," *Journal of Robotic Systems*, vol. 12(6), pp. 417–431, June 1995.

[7] J. P. Ostrowski, *The Mechanics and Control of Undulatory Robotic Locomotion.* PhD thesis, California Institute of Technology, Pasadena, CA, 1995.

[8] J. P. Ostrowski, J. W. Burdick, A. D. Lewis, and R. M. Murray, "The mechanics of undulatory locomotion: The mixed kinematic and dynamic case," in *Proc. IEEE Int. Conf. Robotics and Automation*, (Nagoya, Japan), pp. 1945–1951, May 1995.

[9] A. M. Bloch, P. S. Krishnaprasad, J. E. Marsden, and R. M. Murray, "Nonholonomic mechanical systems and symmetry," 1996. To appear, *Archive for Rational Mechanics and Analysis.*

[10] R. Montgomery, "Isoholonomic problems and some applications," *Communications in Mathematical Physics*, vol. 128(3), pp. 565–592, 1990.

[11] R. M. Murray and S. S. Sastry, "Nonholonomic motion planning: Steering using sinusoids," *IEEE Transactions on Automatic Control*, vol. 38, no. 5, pp. 700–716, 1993.